Proceedings Paper:
Thorn, A., Afacan, D., Ingham, E. et al. (2017) Low-power and low-cost stiffness-variable oesophageal tissue phantom. In: Towards Autonomous Robotic Systems. Towards Autonomous Robotic Systems (TAROS) Conference 2017, 19-21 Jul 2017, Guildford, UK. Lecture Notes in Computer Science , 10454. Springer, pp. 351-362. ISBN: 978-3-319-64106-5. ISSN: 0302-9743. EISSN: 1611-3349.

https://doi.org/10.1007/978-3-319-64107-2

The final publication is available at Springer via http://dx.doi.org/10.1007/978-3-319-64107-2

Low-power and Low-cost Stiffness-variable Oesophageal Tissue Phantom

Alexander Thorn[1*], Dorukhan Afacan[1*], Emily Ingham[2], Can Kavak[1,3], Shuhei Miyashita[4], and Dana D. Damian[1]

[1]Department of Automatic Control and System Engineering, Centre of Assistive Technology and Connected Healthcare, University of Sheffield. Portobello Ln, Sheffield, S1 3JD, United Kingdom. d.damian@sheffield.ac.uk [2]Department of Bioengineering, University of Sheffield. [3]Department of Mechanical Engineering, Izmir Institute of Technology. [4]Department of Electronics, University of York. Alexander Thorn and Dorukhan Afacan contributed equally.

Abstract. Biological tissues are complex structures with changing mechanical properties depending on physiological or pathological factors. Thus they are extendible under normal conditions or stiff if they are subject to an inflammatory reaction. We design and fabricate a low-power and low-cost stiffness-variable tissue phantom (SVTP) that can extend up to 250% and contract up to 5.4% at 5 V (1.4 W), mimicking properties of biological tissues. We investigated the mechanical characteristics of SVTP in simulation and experiment. We also demonstrate its potential by building an oesophagus phantom for testing appropriate force controls in a robotic implant that is meant to manipulate biological oesophageal tissues with changing stiffness in vivo. The entire platform permits efficient testing of robotic implants in the context of anomalies such as long gap esophageal atresia, and could potentially serve as a replacement for live animal tissues.

1 Introduction

We are interested in developing an actuatable phantom oesophagus that will compose a part of our robotic implant system presented in [9]. The robotic implant aims to lengthen oesophageal tissue in vivo for a duration of weeks in order to reconstruct missing oesophageal tissue in the treatment of long-gap oesophageal atresia (LGEA) [10, 11]. During the in vivo performance, the oesophageal tissue experiences not only a change in length as a result of physiological factors, e.g., growth, peristaltic motion [13], but also a change in stiffness, as a consequence of inflammatory responses that are expected in any surgical intervention or implantation over time [7, 6]. It is desired to have an oesophageal phantom capable of mimicking these responses realistically, as a benchtop testing platform for the robotic implant before in vivo evaluation.

In this work, we show the progress in the development of an entirely soft, low-power, low-cost and easy to assemble elastomeric actuator, inspired by [14] where a coiled heat-reactive nylon is introduced, that can be used as a replacement (phantom) for a biological oesophageal tissue (Fig. 1).

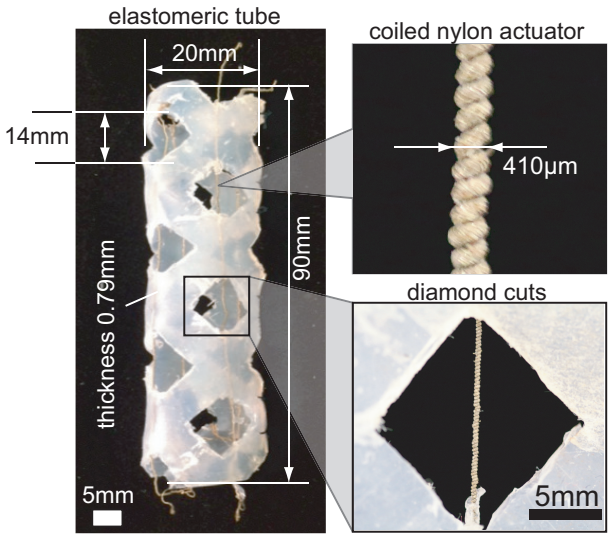

Fig. 1. Elastomeric-embedded coiled actuators as a tubular tissue phantom. Details show the coiled nylon actuator, and a portion of the elastomer with a diamond cut where the a coiled nylon actuator is exposed.

Biological tissues are complex structures with changing mechanical properties depending on physiological or pathological factors. For example, they are soft under normal conditions and stiff if they experience scarring as a result of an inflammatory reaction; or voluntarily alternate states to perform programmed functions, e.g., peristalsis for the oesophagus. As medical robots are playing an increasing role in diagnosis and treatment [31, 23, 30, 18, 24, 3], realistically simulating biological tissues will contribute significantly to the development of efficient medical robots, and replacement or reduction of animal use for in vivo testing.

Although much progress has been achieved in mimicking the physiology of tissue and organs using microchip manufacturing methods [15, 4], contributions to realistic simulation of mechanically-functional biological tissues are limited. Most of the simulation tissues are passive having been used to characterize palpation [22, 8] or for estimating parameters of viscoelastic interactive models of biological tissues during intervention of surgical robots [26, 23].

Soft actuators are most appropriate for building functional structures and robots that mimic the behavior of biological tissues. Challenges in mimicking biological tissues include: (1) extensibility at a large degree; (2) thinness and smoothness; (3) changes in stiffness that do not dramatically change the elastic modulus of the tissue but still maintain its softness; (4) low-cost and low-profile, from the perspective of engineered fabrication.

Muscle-like motion has been achieved most popularly based on pneumatic motion, which is mostly desired for power assisting devices [5, 17, 21, 27, 25].

Shape Memory Alloys (SMA) are also commonly used actuators for controlling stiffness, shape, or vibratory motions, but they would not render it an entirely soft structure [2, 29, 19]. Similar features have also been engineered into polymers [20]. Dielectric elastomer actuators that extend in planar directions provide necessary softness as needed for mimicking biological tissue, though they require considerably high voltage for the attached compliant electrodes [16]. Others soft actuators that can change stiffness are fabricated using a conductive propylene-based elastomer [28] or are driven by an electro-magnetic principle [12]. These technologies all provide advances in compliant actuators, though they are in contradiction to at least one of the properties desirable for building soft tissue phantoms, e.g., require large structures, external pump attachments, or high power consumption.

In this paper, having considered that a challenge resides in realising a medically congruent artificial tissue for in vivo use, we aim to develop a low-power and low-cost stiffness-varying tissue phantom that can support the advancement of in vivo robotic implants. The contributions of this paper are:

1. the concept, design, and fabrication of an active composite material combining thermo-active thread embedded in an elastomer,
2. development of an stiffness variable oesophagus phantom capable of elongation and exhibiting different levels of stiffness,
3. implementation of a varying target force to the closed loop controller depending on the intrinsic properties of the phantom,
4. verification of the proposed model in experiments tested with the robotic implant.

2 Stiffness-Variable Tissue Phantom (SVTP)

2.1 Design

The SVTP is created by embedding coiled nylon actuators [14] in an elastomeric sheet based on a diamond cut stencil (Fig. 1). Given these compounds, this design is entirely soft, exhibiting high stretchability, as well as thermo-electrical contraction, which is similar to how biological tissues function. The fabrication of the SVTP can be low-cost, and easy to fabricate. A reasonable extent of contraction of the SVTP is achieved at the application of low-power, approx 1.4 W for voltages of up to 7 V, making it practical for portable medical device platforms. The diamond-cut stencil embedding the coiled nylon actuator typically reduces the contraction capability as compared with a bare coiled nylon actuator. Nonetheless, this design of the stencil fastens the coil which otherwise would easily curl up around itself rendering it unusable. The cuts where the coil is exposed ensure that the ability of the coil to contract is optimally maintained. Further details of the design on the SVTP are presented in the following sections.

2.2 Coiled Nylon Actuators

The coiled nylon actuators contained within the body of the device contract through its lengthwise axis upon the application of heat [14]. These actuators are made of a Shieldex 117/17 dtex 2-ply HC+B wire (Statex Produktions + Vertriebs GmbH) which is a nylon multi-filament yarn coated in silver. Contraction can also be obtained using a coil of bare nylon wire. The actuator is fabricated by hanging the wire from the shaft of a motor with a weight of 68.3 g attached to the other end, keeping the yarn taut. The weight is restricted from rotation and the motor is powered to induce twists into the fibre eventually resulting in a coil forming around itself into a spring-like shape. It was found that the Shieldex yarn had a coiling ratio of 4:1 whereby the original wire becomes its length once fully coiled. These coils are to be tested using a heat gun to prove that they can contract lengthwise under heat. This process also requires the untwisting of the coils under a weight of 16 g until they lift this weight by a minimum of 1 cm. This process of coil fabrication is easily carried out and requires minimal equipment.

2.3 Fabrication of SVTP

The process of fabrication is illustrated in Fig. 2. The SVTP is fabricated by moulding Ecoflex 00-10 (Smooth On) embedded with coiled nylon actuators, according to a checkerboard stencil with a diamond orientation. This stencil is fabricated from sheets of plain paper and double-sided acrylic adhesive sheets in an alternating order. The checkerboard design is either hand-cut or laser-cut (LS6840 Laser Engraving Machine, Laserscript). The latter version provides a neater finish to the checkerboard stencil. This layout features squares of $1 \times 1\,\mathrm{cm}^2$ separated by bridges of $0.2 \times 1\,\mathrm{cm}^2$. Four alternative sheets of paper and adhesive stencils are placed in a container ($11.8 \times 20.5\,\mathrm{cm}^2$ (length$\times$width)). The first layer of adhesive sheet ensures that the template is well held in the container. Pre-prepared coiled nylon actuators (length 10.5 cm, diameter 0.41 mm) are placed in a taut configuration along each column of diamonds over this template. Subsequently, a top template consisting of a layer of adhesive sheet and a layer of paper is placed on top. This layer of adhesive ensures that the coiled nylon actuators are kept in place above the lower template. The checkerboard stencil design has the purpose of exposing the coiled nylon actuators in diamond-shape cuts. The two templates (bottom and top) that sandwich the actuators ensure that they are well embedded in the target elastomeric structure. Once the template and the coil actuators are firmly in place, the bridges between the squares are manually removed from the container. Finally, an even layer of Ecoflex 00-10 is poured in the gaps with a thickness equal to that of the overall template (0.79 mm) and takes approximately 4 hours to set. Once fully set, the contents of the tray are removed and the paper is manually extracted from the elastomeric sheet to produce the SVTP. The resulting sheet is folded into a cylinder by connecting the two edges parallel to the coils using Ecoflex 00-10 or silk surgical sutures.

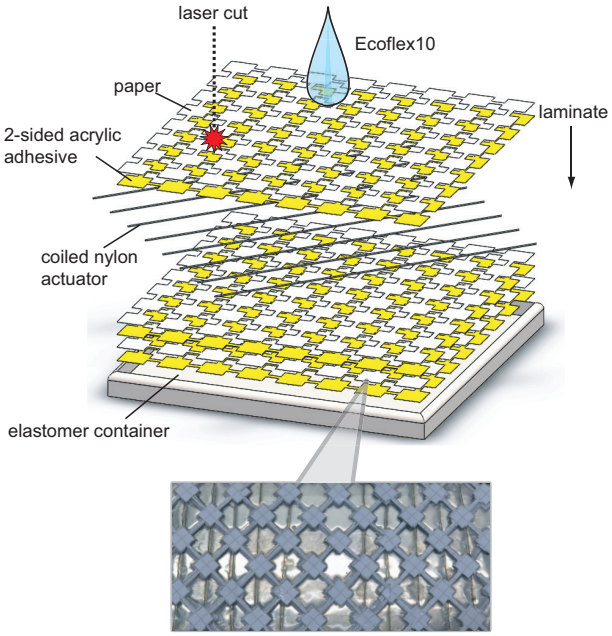

Fig. 2. Fabrication process of SVTP. Laminated layers of paper and double-sided acrylic adhesive sheets sandwich coiled nylon actuators. A checkerboard stencil with a diamond orientation is used to control the exposure of the coiled nylon actuators outside of an elastomeric substrate that is poured into the stencil structure.

2.4 Finite Element Analysis of SVTP Contraction

We have analyzed the deformation of the SVTP by a given force input from a single coiled nylon actuator using finite element method (FEM) analysis. The simulated structure was a model of a single section of the SVTP containing one diamond cut spanning $20 \times 20 \times 1.4\,\mathrm{mm}^3$.

Fixed support was added to the top and the bottom faces of the section, and an experimentally obtained value of the initial shear modulus of elastomer, $G = 920.6\,\mathrm{Pa}$, was used. Forces were applied to the top and the bottom corner of the cut at at magnitude of 0.08 N toward the bottom and 0.08 N toward the top, along the vertical axis, respectively. Commercially available software (Ansys) was used for analysis.

Figure 3 (a) shows the result of the analysis. The maximum deformation of 3.85 mm was yielded under these circumstances.

Figure 3 (b)(c) shows before and after the contraction of SVTP comprising 4 columns of diamond cuts and thus 4 coiled nylon actuators involved to produce force. A value of 16.33 g was experimentally applied (0.082 N at each end of the diamond) which is comparable to the condition in Fig. 3 (a). The observed contraction was about 3 mm which is 72% of the value predicted in FEM analysis.

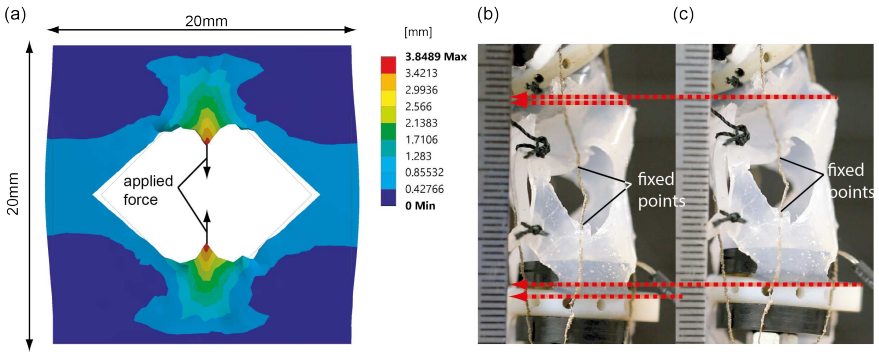

Fig. 3. Contraction of the SVTP. FEM analysis of the contraction of one section of SVTP induced by a coiled nylon actuator (a), experimental result of contraction with four coiled nylon actuator before force is applied (b) and after force is applied (c).

2.5 Robotic Implant

The SVTP assembled as an oesophagus phantom is a reliable platform to test the adaptive force control of a robotic implant, before it is used in vivo on biological tissue. The implant is a 1-DOF linear actuator Fig.4. Prototype design is taken from [9] targeting 2-year-old patients of (LGEA), for which treatment of tissue reconstruction requiring the application of mechanical stimulation to the tissue. The device uses two suspender rings to attach to the oesophagus phantom, and applies traction to the tissue by gap adjustment between the suspender rings using a DC motor connected to a worm gear. It is equipped with two sensors: (1) Force sensor (FS Series, Honeywell) whose signal is amplified by a non-inverting differential amplifier (MCP6004, Microchip). (2) K-type thermocouple whose signal is amplified by Adafruit MAX31855 amplifier and transmitted via SPI communication protocol. An Atmega 328 microcontroller (Baby Orangutan, Pololu) is used to receive force sensor and thermocouple feedback.

2.6 Robot Implant's Control

Direct force control is implemented to manipulate the traction force applied on the oesophageal phantom by actuating the suspender ring. The robotic implant and the oesophageal phantom are holistically brought together and regarded as a single plant since there is no non-contact to contact transition. The unpredictable tissue mechanics induce uncertainty to the plant structure, and as a result the controller design relies on identification of the plant model. Model identification adaptive control previously yielded that the holistic approach is plausible as the tissue mechanics affect the implant behaviour with the reaction force as the elastomeric structure elongates [1]. After system identification trials under a step input, which approximated the plant as a first order system, a PI force controller is implemented on the plant by adjusting the force controller gains for

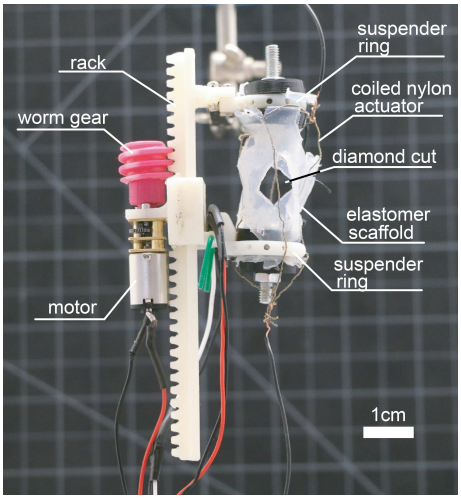

Fig. 4. The robotic implant setup with a 4-coil tubular SVTP.

the desired over damped behaviour. The tissue adaptive capability of the implant was furthered by stiffness based adjustment of target force being provided to the tuned controller.

3 Experimental Results

3.1 Experimental Procedure for Measuring SVTP Stiffness

In order to extract the characteristics of the SVTP an experimental setup and procedure for testing the compression were established. The oesophagus phantom was thermo-electrically actuated through Joule heating from a power source in which the voltage was gradually increased in steps of 1 volt. At each step, the heat was distributed uniformly along the actuator with maximum differences of 2°C. As the coil acts as a resistor the increase in voltage increases the current and results in a higher heat and a lengthwise contraction of the coil. The SVTP was then extended by adding weights until the coil returned to its original length showing the force of the contraction. This process of heating was limited to an experimentally found maximum, as higher voltages resulted in an increased chance of structural damage in the coiled nylon actuator. The contraction of the tubular structure is reflected in a temperature change which is acquired by the thermocouple.

3.2 One-coil SVTP Comparative Stiffness

Fig. 5 shows the comparative differences in stiffness performance of a bare coiled nylon actuator as shown in [14], a coiled nylon actuator embedded in plain

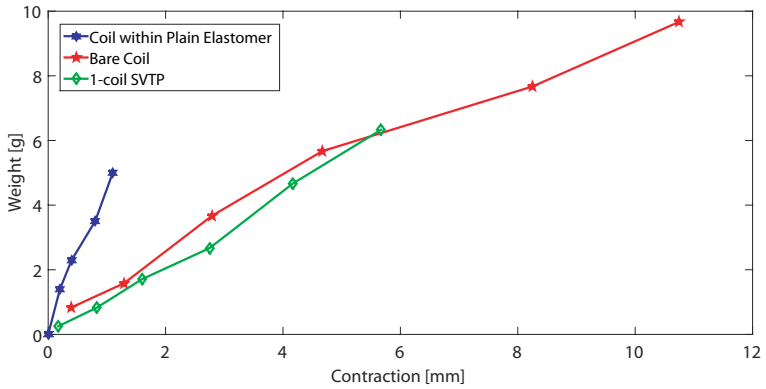

Fig. 5. The results of averaging 3 trials of compression for three separate individual coiled nylon actuators within either no elastomer (red), a plain elastomer sheet coating (blue) or an SVTP coating (green).

elastomeric sheet, and a one-coil SVTP. In this experiment coiled nylon actuators of length $10 - 10.5$ cm were used. The elastomer sheets had an average length of 9.45 cm, width of 2.3 cm and thickness of 0.98 cm. The SVTP had 57% of its coil exposed outside the elastomer. When the maximum voltage of 6 V is applied to each end of the coil (a maximum of 5 V for the coiled nylon actuator embedded in a plain elastomeric sheet), the average maximum contraction ranges up to $10 - 11$ mm and a temperature maximum ranges within $50 - 60$ °C. The resistance of each individual coil varied with average values of 69.1 ohms, 50.75 ohms and 71.4 ohms,for the bare coiled nylon actuator, the actuator embedded in plain elastomeric sheet and the SVTP samples.

It can be seen that placing a coil within a flat plain sheet of elastomer resulted in a large degradation in performance whereas the diamond cut structure performs in proportion to the bare coil with regards to the amount of exposed coil length. It showed 52.7% of the average maximum contraction and held 65.5% of the maximum weight compared to the exposed coil. The deviations from the proportionality can be explained by taking into account errors relating to humans in experimentation and manufacturing errors during coiling.

3.3 Oesophagus Phantom Stiffness

In Fig. 6 the compression outcome resulting from experiments as described in Section IIIA are shown for the SVTP prototype. This SVTP contains within it 3 coils of 8 cm average total length whereas 5.5 cm of it(68.8% ratio) is the average length exposed outside. They had an average total resistance of 39.4 ohms and had a maximum 7 volts applied across them. It can be seen that the average maximum contraction is 2.1% of its total length. This takes the coils to a maximum temperature range $37 - 46$°C.

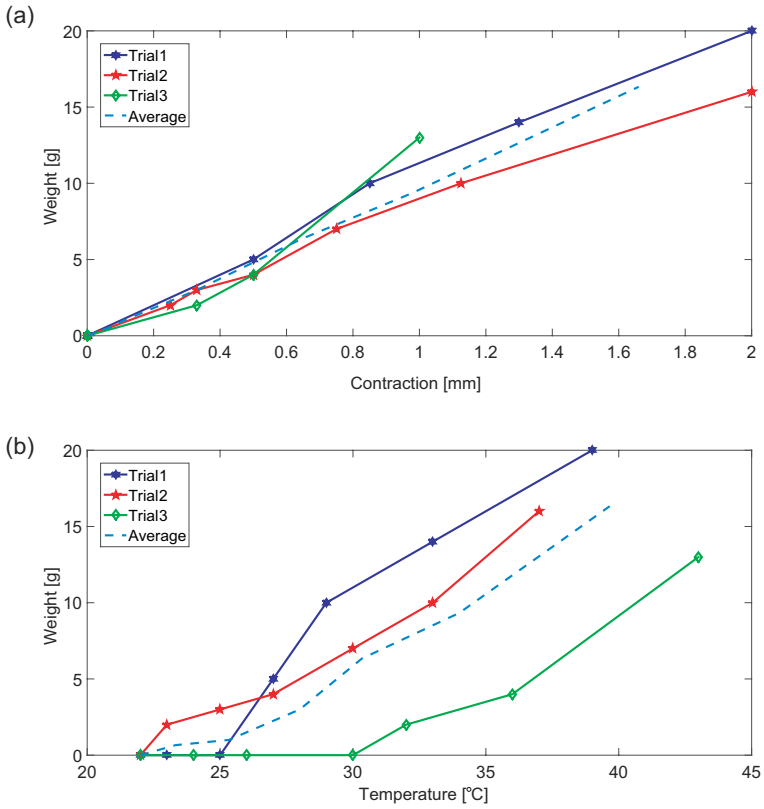

Fig. 6. Contraction vs weight vs temperature for a 3-coil SVTP.

3.4 Force Control of Oesophageal Phantom

During oesophageal lengthening treatment, tissue length and stiffness are subject to change and thus uncertain. As the tissue gets stiffer or as it contracts with peristaltic motion, it will apply a higher reaction force on the implant ring, elongating it. Thus lowering the target force can induce a compliant behaviour in the presence of such unpredictable occurrences. As a result, the target force is set depending on the stiffness of the oesophageal phantom. A 4-coil SVTP is incorporated to robotic implant platform seen in Fig. 4. The information about the reaction force is obtained from the temperature change of the coiled nylon actuators in the oesophageal phantom as current passes through them. As the temperature increases while the coiled nylon actuators contract, the increase in the force applied by the oesophagus phantom (F_e) is accounted as the reaction force induced by the increasing stiffness. Computed F_e is used to define a new target force based on an inversely proportional affine relationship in each iteration of the controller with the function

$$F_{target} = 0.6 - 25\,F_e, \tag{1}$$

where the target force is bounded by 0.6 N to avoid damage to SVTP and the coils. The response of the robotic implant to the varying stiffness of the esophagus phantom is shown in Fig. 7.

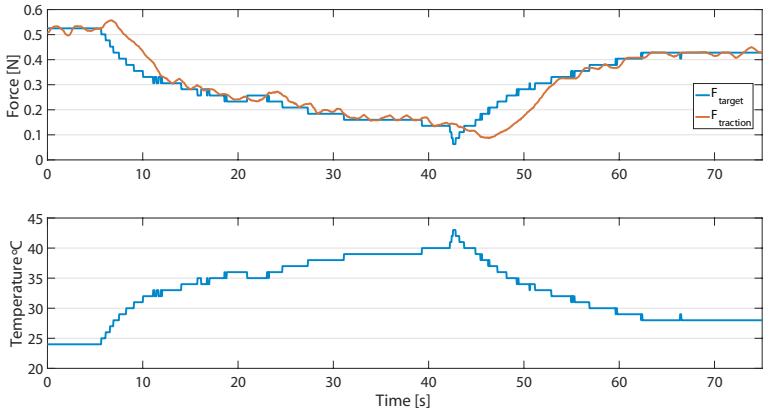

Fig. 7. Elastomer scaffold contracts increasing the overall stiffness. This induces a reaction force and an increase in the temperature of the coiled nylon actuators. Target force changes with respect to the temperature. Traction force response follows the target force with overdamped convergence.

4 Discussion & Conclusion

This work presents an energy efficient, low-profile tissue phantom whose stiffness or length can be varied. The developed phantom, SVTP, jointly with the robotic implant poses a desirable aid for the bench top synthesis of a tissue stiffness adaptive force controller of the implant for oesophageal atresia treatment. The elastomer structure forms a casing around the coiled nylon actuators, sheltering them from damage and also encouraging their elongation. It also does this with proportional stroke length and force to the amount of coil exposed. The implemented controller has been enhanced to produce a desired target force that will also contribute to avoiding tissue damage during elongation.

The method of electrical actuation of SVTP using low power consumption to achieve reasonable contractions is suitable to develop portable applications for in vivo medicine. These contractions were yielded at body temperatures which make the SVTP a candidate for in vivo tissue manipulation.

The current limitation of the proposed oesophageal phantom is that while it can change the stiffness and the length, both features cannot be altered at

the same time. The capability of changing these properties simultaneously is a desired feature in order to simulate both induced tissue growth and stiffness changes.

Another constraint is the magnitude of achievable contraction with the given power. While this is sufficient for the purpose of designing force controls with a qualitative value, the actuators should allow a broader range of contraction in order to more accurately mimic specific properties of biological tissues.

In this respect, future work includes increasing the stroke length that could be undertaken by following [14] further to create coils with a larger Spring Index (the ratio between the coil and fibre diameter). We also plan to embed soft sensors in the tissue phantoms in order to build a complete robotic structure, and to advance the soft robot to full biocompatibility such that it can also function as an implant in vivo.

Acknowledgment

We thank Emily Southern for her help with the paper revision. This work was supported by the University of Sheffield.

References

[1] D. Afacan. "Stiffness-adaptive Control of Tissue Manipulation using a Robotic Implant". MA thesis. Sheffield, UK: University of Sheffield, 2016.

[2] B.S. Balapgol, S.A. Kulkarni, and K.M. Bajoria. "A review on shape memory alloy structures". In: *International Journal of Acoustics and Vibration* 9(2) (2004), pp. 6117–68.

[3] C. Bergeles and Y. Guang-Zhong. "From Passive Tool Holders to Microsurgeons: Safer, Smaller, Smarter Surgical Robots". In: *IEEE Trans. Biomed. Eng* 61(5) (2014), pp. 1565–76.

[4] S. N. Bhatia and D. E. Ingber. "Microfluidic organs-on-chips". In: *Nature Biotechnology* 32 (2014), pp. 760–772.

[5] D. G. Caldwell, G. Medrano-Cerda, and M. Goodwin. "Control of pneumatic muscle actuators". In: *IEEE Control Systems Magazine* 15(1) (1995), pp. 4017–48.

[6] R. H. Cartabuke, R. Lopez, and P. N. Thota. "Long-term Esophageal and Respiratory Outcomes in Children with Esophageal Atresia and Tracheoesophageal Fistula". In: *Oxford Journals, Medicine and Health, Gastroenterology Report* (2015), pp. 1–5.

[7] D. T. Corr and D. A. Hart. "Biomechanics of Scar Tissue and Uninjured Skin". In: *Adv Wound Care (New Rochelle)* 2(2) (2013), pp. 37–43.

[8] I. F. Costa. "A novel deformation method for fast simulation of biological tissue formed by fibers and fluid". In: *Medical Image Analysis* 16(5) (2012), pp. 1038–1046.

[9] D. D. Damian et al. “Robotic Implant to Apply Tissue Traction Forces in the Treatment of Esophageal Atresia”. In: *IEEE International Conference on Robotics and Automation (ICRA)*. 2014, pp. 786–792.

[10] J. E. Foker et al. “Development of a true primary repair for the full spectrum of esophageal atresia.” In: *Annals of Surgery* 226(4) (1997), pp. 533–543.

[11] J. E. Foker et al. “Long-gap esophageal atresia treated by growth induction: the biological potential and early follow-up results”. In: *Seminars in Pediatric Surgery* 18 (2009), pp. 23–29.

[12] F. Fries et al. “Electromagnetically Driven Elastic Actuator”. In: *International Conference on Robotics and Biomimetics*. 2014, pp. 309–314.

[13] R. K. Goyal and A. Chaudhury. “Physiology of Normal Esophageal Motility”. In: *Journal of Clinical Gastroenterology* 42(5) (2008), pp. 610–619.

[14] C. Haines et al. “Artificial Muscles from Fishing Line and Sewing Thread”. In: *Science* 343 (2014), pp. 868–872.

[15] D. Huh, G. A. Hamilton, and D. E. Ingber. “From Three-Dimensional Cell Culture to Organs-on-Chips”. In: *Trends Cell Biology* 21(12) (2011), pp. 745–754.

[16] K. Jung, K. J. Kim, and H. R. Choi. “Self-sensing of dielectric elastomer actuator”. In: *Sensors Actuators A: Physical* 143 (2008), pp. 343–351.

[17] G. K. Klute, J. M. Czerniecki, and B. Hannaford. “Mckibben artificial muscles: Pneumatic actuators with biomechanical intelligence”. In: *IEEE/ASME International Conference on Advanced Intelligent Mechatronics*. 1999, pp. 221–226.

[18] M. P. Kummer et al. “OctoMag: An Electromagnetic System for 5-DOF Wireless micromanipulation”. In: *IEEE International Conference on Robotics and Automation (ICRA)*. 2010, pp. 1006–1017.

[19] C. Laschi et al. “Soft robot arm inspired by the octopus”. In: *Advanced Robotics* 26.7 (2012), pp. 709–727.

[20] A. Lendlein and S. Kelch. “Shape-memory polymers”. In: *Angew. Chem. Int. Ed.* 41 (2002), pp. 2034–172057.

[21] R. V. Martinez et al. “Elastomeric Origami: Programmable Paper-Elastomer Composites as Pneumatic Actuators”. In: *Advanced Functional Materials* 22 (2012), pp. 1376–1384.

[22] S. Misra, K. Ramesh, and A. M. Okamura. “Modeling of Nonlinear Elastic Tissues for Surgical Simulation”. In: *Computer methods in biomechanics and biomedical engineering* 13(6) (2010), pp. 811–818.

[23] S. Miyashita et al. “Ingestible, Controllable, and Degradable Origami Robot for Patching Stomach Wounds”. In: *IEEE International Conference on Robotics and Automation (ICRA)*. 2016.

[24] B. J. Nelson, I. K. K., and J. J. Abbott. “Microrobots for Minimally Invasive Medicine”. In: *Annual Review of Biomedical Engineering* 12 (2010), pp. 55–85.

[25] K. Ogawa, K. Narioka, and K. Hosoda. “Development of whole-body humanoid ”pneumat-BS” with pneumatic musculoskeletal system”. In: *IEEE/RSJ*

International Conference on Intelligent Robots and Systems. 2011, pp. 4838–4843.

[26] J. Palacio-Torralba et al. "Quantitative diagnostics of soft tissue through viscoelastic characterization using time-based instrumented palpation". In: *Journal of the Mechanical Behavior of Biomedical Materials* 41 (2015), pp. 149–160.

[27] E. T. Roche et al. "A Bioinspired Soft Actuated Material". In: *Advanced Materials* 26(8) (2014), pp. 1200–1206.

[28] W. Shan et al. "Rigidity-tuning conductive elastomer". In: *Smart Materials and Structures* 24(6) (2015), pp. 343–351.

[29] T. Umedachi, V. Vikas, and B. A. Trimmer. "Softworms: The Design and Control of Non-pneumatic, 3D-Printed, Deformable Robots". In: *Bioinspiration & Biomimetics* 11 (2016), p. 025001.

[30] P. Valdastri, M. Simi, and R. J. Webster III. "Advanced Technologies for Gastrointestinal Endoscopy". In: *Annual Review of Biomedical Engineering* 14 (2012), pp. 397–429.

[31] S. Yim, K. Goyal, and M. Sitti. "Magnetically Actuated Soft Capsule With the Multimodal Drug Relase Function". In: *IEEE/ASME Transactions on Mechatronics* 18.4 (2013), pp. 1413–1418.